

SLIP EFFECTS ON FLOW, HEAT, AND MASS TRANSFER OF NANOFLUID OVER STRETCHING HORIZONTAL CYLINDER IN THE PRESENCE OF SUCTION/INJECTION

by

**Elsayed M. A. ELBASHBESHY^a, Tarek G. EMAM^a, Magdi S. El-AZAB^b,
and Khaled M. ABDELGABER^{*c}**

^a Mathematics Department, Faculty of Science, Ain Shams University, Abbassia, Cairo, Egypt

^b Department of Physics & Engineering Mathematics, Faculty of Engineering,
Mansoura University, Mansoura, Egypt

^c Department of Physics & Engineering Mathematics, Faculty of Engineering – Mataria,
Helwan University, Cairo, Egypt

Original scientific paper
DOI: 10.2298/TSCI140512135E

Two slip effects, Brownian diffusion and thermophoresis, on flow, heat, and mass transfer of an incompressible viscous nanofluid over a stretching horizontal cylinder in the presence of suction/injection are discussed numerically. The governing boundary layer equations are reduced to a system of ordinary differential equations. MATHEMATICA has been used to solve such system after obtaining the missed initial conditions. Comparison of obtained numerical results is made with previously published results in some special cases and found to be in a good agreement.

Key words: laminar flow, boundary layer, stretching horizontal cylinder,
Brownian diffusion, thermophoresis, nanofluid

Introduction

The problem of boundary layer flow and heat transfer over a moving or stretching surface is of interest in numerous industrial applications such as polymer extrusion processes, hot rolling, paper production, wire drawing, aerodynamic extrusion of plastic sheets, and condensation process of metallic plate in a cooling bath and glass.

In 1904, Prandtl proposed the boundary layer theory which states that the viscous effects would be confined to thin shear layers adjacent boundaries in the case of the motion of fluids with very little viscosity [1]. So the motion of the surface through the fluid creates a boundary layer whose thickness grows with increasing distance from the hole out of which the surface issues. The evaluation of heat transfer rates depend on knowledge of this boundary layer.

The boundary layer behaviour on moving surfaces in a viscous fluid at rest is considered by Sakiadis [2, 3]. The dynamics of the boundary layer flow over a stretching surface originated from the pioneering work of Crane [4]. He studied a steady 2-D incompressible boundary layer flow due to a moving stretching surface with a constant surface temperature in an ambient fluid also considered the case when the velocity varies linearly with the distance from a fixed point and gave a similarity solution in a closed analytical form. The work of Sakiadis and Crane was subsequently extended by [5-27].

* Corresponding author; e-mail: dr.khaledabdelgaber@hotmail.com

The conventional heat transfer fluids including oil, water, and ethylene glycol mixture are poor heat transfer fluids. Recently, a new fluid called nanofluid has been used to improve the heat transfer properties of the conventional one. Masuda *et al.* [28] suggested that the suspension of nanoparticles in the conventional fluid improves its thermal conductivity which plays an important role on the heat transfer between the medium and the surface. Choi [29] is the first who used the term *nanofluid* to refer to a conventional fluid (base) which contains very tiny solid particles (nanoparticles). The addition of a small amount (less than 1% by volume) of nanoparticles to conventional fluids increased the thermal conductivity of the fluid up to approximately two times as showed by Choi *et al.* [30].

The nanoparticle absolute velocity can be viewed as a sum of the base fluid velocity and a relative (slip) velocity, as mentioned by Buongiorno [31]. There are several slip mechanisms by which the nanoparticles can develop a slip velocity, *e.g.*, inertia, Brownian diffusion, thermophoresis, diffusiophoresis, Magnus effect, fluid drainage, and gravity settling. Brownian diffusion is a random diffusion of nanoparticles within the base fluid due to the continuous collisions between the nanoparticles and the molecules of the base fluid while thermophoresis is a random diffusion of nanoparticles within the base fluid under the effect of a temperature gradient. Brownian and thermophoresis diffusions play a crucial role in many applications, *e.g.*, filters, particle deposition on boilers, and different measurement techniques for aerosols during combustion. The work of Masuda and Choi was subsequently extended by [32-43].

In the present work, effects of two slip motions, Brownian diffusion and thermophoresis, on flow, heat, and mass transfer of an incompressible viscous nanofluid over a stretching horizontal cylinder in the presence of suction/injection are discussed numerically. The similarity solutions may be obtained by assuming that the cylinder is stretched with linear velocity in the axial direction.

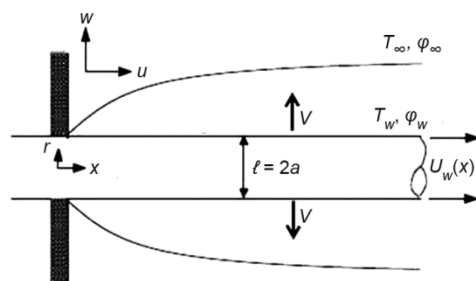


Figure 1. Physical model and co-ordinate system

Mathematical formulation

Consider a steady and axisymmetric boundary layer flow of an incompressible viscous nanofluid along a continuously stretching horizontal cylinder of radius, a , as shown in fig. 1. The cylinder is being stretched and the nanofluid is being moved along the axial direction, x . The radial co-ordinate, r , is perpendicular to the cylinder axis. The nanofluid has the linear velocity $U_w(x) = U_0 x / \ell$, the constant temperature, T_w , and the constant concentration, φ_w , along the stretching surface.

The continuity, momentum, and energy equations governing such type of flow will be written in the following mathematical model [28, 32, 40]:

$$\frac{\partial}{\partial x} (r u) + \frac{\partial}{\partial r} (r v) = 0 \quad (1)$$

$$u \frac{\partial u}{\partial x} + v \frac{\partial u}{\partial r} = \frac{\mu}{\rho r} \frac{\partial}{\partial r} \left(r \frac{\partial u}{\partial r} \right) \quad (2)$$

$$u \frac{\partial T}{\partial x} + v \frac{\partial T}{\partial r} = \frac{\alpha}{r} \frac{\partial}{\partial r} \left(r \frac{\partial T}{\partial r} \right) + \frac{(\rho C)_p}{\rho C} \left[D_B \left(\frac{\partial \varphi}{\partial x} \frac{\partial T}{\partial x} + \frac{\partial \varphi}{\partial r} \frac{\partial T}{\partial r} \right) + \frac{D_T}{T_\infty} \left(\frac{\partial \varphi}{\partial x} \frac{\partial T}{\partial x} + \frac{\partial \varphi}{\partial r} \frac{\partial T}{\partial r} \right) \right] \quad (3)$$

$$u \frac{\partial \phi}{\partial x} + v \frac{\partial \phi}{\partial r} = \frac{D_B}{r} \frac{\partial}{\partial r} \left(r \frac{\partial \phi}{\partial r} \right) + \frac{D_T}{T_\infty r} \frac{\partial}{\partial r} \left(r \frac{\partial T}{\partial r} \right) \quad (4)$$

subject to the boundary conditions:

$$u = U_w(x), \quad v = V, \quad T = T_w, \quad \phi = \phi_w, \quad \text{at } r = a, \quad (5)$$

$$u \rightarrow 0, \quad T \rightarrow T_\infty, \quad \phi \rightarrow \phi_\infty, \quad \text{as } r \rightarrow \infty \quad (6)$$

where V is the uniform velocity of suction ($V < 0$) or injection ($V > 0$).

The continuity equation is satisfied if a stream function, $\psi(x, r)$, is chosen such that $u = r^{-1} \partial \psi / \partial r$ and $v = -r^{-1} \partial \psi / \partial x$. The similarity transformations:

$$\eta = \frac{r^2 - a^2}{2a} \sqrt{\frac{U_w}{vx}}, \quad \psi(x, r) = a \sqrt{U_w vx} f(\eta), \quad \theta(\eta) = \frac{T - T_\infty}{\Delta T}, \quad \phi(\eta) = \frac{\phi - \phi_\infty}{\Delta \phi}$$

are substituted into eqs. (2)-(4) to obtain the following system of ordinary differential equations:

$$(1 + 2\gamma\eta) f''' + (2\gamma + f) f'' - f'^2 = 0 \quad (7)$$

$$(1 + 2\gamma\eta) \theta'' + (2\gamma + \text{Pr}f) \theta' + \text{Pr}(1 + 2\gamma\eta) (N_B \phi' + N_T \theta') \theta' = 0 \quad (8)$$

$$N_B [(1 + 2\gamma\eta) \phi'' + (2\gamma + \text{Sc}f) \phi'] + N_T [(1 + 2\gamma\eta) \theta'' + 2\gamma\theta'] = 0 \quad (9)$$

subject to the boundary conditions:

$$f(0) = -f_0, \quad f'(0) = 1, \quad \theta(0) = 1, \quad \phi(0) = 1, \quad (10)$$

$$f'(\infty) \rightarrow 0, \quad \theta(\infty) \rightarrow 0, \quad \phi(\infty) \rightarrow 0, \quad (11)$$

where primes denote differentiation with respect to η , $\Delta T = T_w - T_\infty$, $\Delta \phi = \phi_w - \phi_\infty$, $\gamma = a^{-1} (v\ell/U_0)^{1/2}$ is the curvature parameter, $\text{Pr} = v/\alpha$ – the Prandtl number, $N_B = (\rho C_p D_B \Delta \phi / \rho C)$ – the Brownian diffusion parameter, $N_T = (\rho C_p D_T \Delta T / \rho C T_\infty)$ – the thermophoresis parameter, $\text{Sc} = D_B/v$ – the Schmidt number, and $f_0 = (\ell/v U_0)^{1/2} V$ – the suction ($f_0 < 0$) or injection ($f_0 > 0$) parameter.

The physical quantities of interest here are the skin friction coefficient, C_f , the local Nusselt number, Nu_x , and the local Sherwood number, Sh_x which are defined:

$$C_f = \frac{2\tau_w}{\rho U_w^2}, \quad \text{Nu}_x = \frac{x q_w}{\kappa \Delta T}, \quad \text{Sh}_x = \frac{x Q_w}{\kappa \Delta \phi} \quad (12)$$

where $\tau_w = -\mu (\partial u / \partial r)_{r=a}$ is the surface shear stress, $q_w = -\kappa (\partial T / \partial r)_{r=a}$ – the surface heat flux, and $Q_w = -D_B (\partial \phi / \partial r)_{r=a}$ – the surface mass flux. Substituting the similarity transformations into eq. (12) yields:

$$\frac{1}{2} C_f \sqrt{\text{Re}} \bar{x} = -f''(0), \quad \frac{\text{Nu}_x}{\sqrt{\text{Re}}} \bar{x} = -\theta'(0), \quad \frac{\text{Sh}_x}{\sqrt{\text{Re}}} \bar{x} = -\phi'(0) \quad (13)$$

where $\bar{x} = \sqrt{x/\ell}$ and $\text{Re} = \ell U_w / v$.

Numerical solution

Equations (7)-(9) subject to the boundary conditions, eqs. (10) and (11), are converted into the following simultaneous system of first order differential equations:

$$y'_1 = y_2, \quad y'_2 = y_3, \quad y'_4 = y_5, \quad y'_6 = y_7 \quad (14)$$

$$y'_3 = \frac{1}{1+2\gamma\eta} [-(2\gamma + y_1)y_3 + y_2^2] \quad (15)$$

$$y'_5 = -\frac{1}{1+2\gamma\eta} (2\gamma + \text{Pr} y_1)y_5 - \text{Pr}(N_B y_7 + N_T y_5)y_5 \quad (16)$$

$$y'_7 = -\frac{1}{1+2\gamma\eta} (2\gamma + \text{Sc} y_1)y_7 - \frac{N_T}{N_B} \left(y'_5 + \frac{2\gamma}{1+2\gamma\eta} y_5 \right) \quad (17)$$

where $y_1 = f(\eta)$, $y_4 = \theta(\eta)$, and $y_6 = \phi(\eta)$. The initial conditions are:

$$y_1(0) = -f_0, \quad y_2(0) = 1, \quad y_3(0) = s_1, \quad y_4(0) = 1, \quad y_5(0) = s_2, \quad y_6(0) = 1, \quad y_7(0) = s_3 \quad (18)$$

where s_1 , s_2 , and s_3 are priori unknowns to be determined as a part of the solution.

By using MATHEMATICA, a function $F(s_1, s_2, s_3)$ is defined by NDSolve command. One of them used here is the efficient pair of explicit Runge-Kutta formulas of order 4 and 5 (RKBS45) derived by Bogacki and Shampine [44]. The values of s_1 , s_2 , and s_3 are determined upon solving the equations, $y_2(\eta_{\max}) = 0$, $y_4(\eta_{\max}) = 0$, and $y_6(\eta_{\max}) = 0$. A suitable value of η is taken and then increased to reach η_{\max} such that the difference between two successive values of s_1 , those of s_2 , and those of s_3 is less than 10^{-6} . Once the unknowns s_1 , s_2 , and s_3 are determined, the system is closed and is solved numerically again using NDSolve to get the final results.

Results

The computations have been carried out for various values of the previously defined parameters γ , Pr , N_B , N_T , Sc , and f_0 . The accuracy of the numerical scheme is checked out by performing various comparisons at different conditions with previously published papers. The values of the modified Nusselt number, $-\theta'(0)$, are compared with those reported in [13, 35] and are found to be in a good agreement as shown in tab. 1.

Table 1. Comparison of $-\theta'(0)$ for various values of Pr when $\gamma = N_T = N_B = \text{Sc} = f_0 = 0$

Pr	Wang [13]	Khan and Pop [35]	Present results
0.2	0.1691	0.1691	0.169088575
0.7	0.4539	0.4539	0.453916156
2	0.9114	0.9114	0.911357700
7	1.8954	1.8954	1.895403259
20	3.3539	3.3539	3.353904216
70	6.4622	6.4622	6.4621996188

The effects of γ , Pr, N_B , N_T , Sc, and f_0 on the cylinder surface physical quantities, $-f''(0)$, $-\theta'(0)$, and $-\phi'(0)$, are listed in tab. 2.

Table 2. The values of $-f''(0)$, $-\theta'(0)$, and $-\phi'(0)$ for various values of parameters

γ	Pr	N_B	N_T	Sc	f_0	$-f''(0)$	$-\theta'(0)$	$-\phi'(0)$
1	5	0.5	0.2	0.5	0	1.34321	0.87071	0.43978
2						1.64795	0.85923	0.79232
3						1.92971	0.87093	1.11613
5						2.45107	0.91628	1.72047
10						3.62166	1.04857	3.12157
2	1	0.5	0.2	0.5	0	1.64795	0.84246	0.77329
	5					1.64795	0.85923	0.79232
	7					1.64795	0.75641	0.83706
	10					1.64795	0.60054	0.90204
2	5	0.2	0.2	0.5	0	1.64795	1.26423	0.40916
		0.5				1.64795	0.85923	0.79232
		1				1.64795	0.34145	0.92506
		2				1.64795	0.03000	0.92068
2	5	0.5	0.2	0.5	0	1.64795	0.85923	0.79232
			0.5			1.64795	0.57052	0.93223
			1			1.64795	0.28105	1.48007
			2			1.64795	0.06712	2.64708
2	5	0.5	0.2	0.2	0	1.64795	1.02970	0.52238
				0.5		1.64795	0.85923	0.79232
				1		1.64795	0.67316	1.14498
				2		1.64795	0.49298	1.61139
2	5	0.5	0.2	0.5	-1 -0.5 0 0.5 1	2.16835 1.89344 1.64795 1.43075 1.24018	3.24253 1.84573 0.85923 0.31409 0.08986	0.07053 0.51429 0.79232 0.88881 0.85529

It is obvious that the value of the skin friction coefficient, $-f''(0)$, is positive for all values of the different parameters. Physically, the positive value of $-f''(0)$ means the surface exerts a drag force on the nanofluid which is suitable for our present problem because the stretching cylinder will induce the nanofluid flow. Finally, the effects of γ , Pr, N_B , N_T , Sc, and f_0 on the nanofluid velocity, temperature, and concentration are illustrated in figs. 2-15.

Discussions

The effects of curvature, Prandtl number, Brownian diffusion, thermophoresis diffusion, Schmidt number, and suction/injection velocity on the nanofluid velocity, temperature, and concentration profiles and on the cylinder surface shear stress, and heat flux are discussed further in the paper.

Curvature

It is observed from tab. 2 that the surface shear stress (skin friction), mass flux (Sherwood number), and heat flux (Nusselt number) increase by increasing the curvature parameter, γ . Good explanation of these observations is that the increase of γ results in decreasing the surface area of the cylinder.

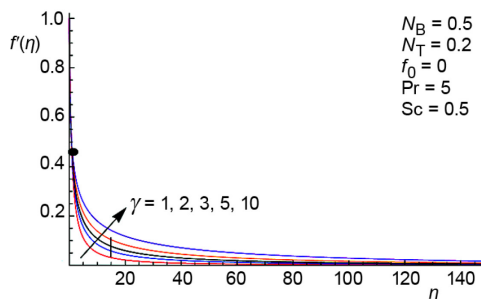


Figure 2. The velocity profiles for various values of γ

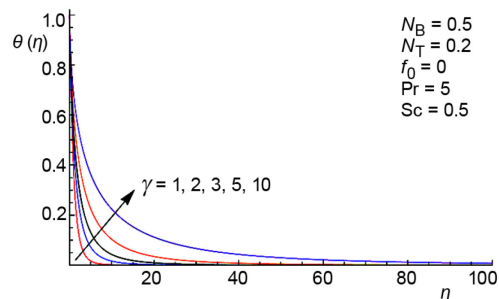


Figure 3. The temperature profiles for various values of γ

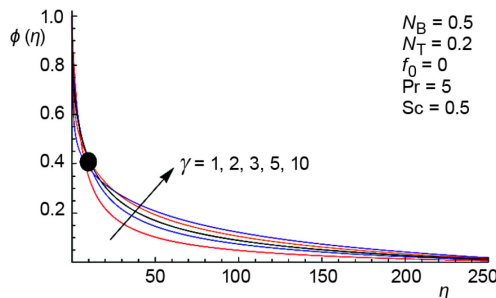


Figure 4. The concentration profiles for various values of γ

velocity to be a free stream is enhanced by increasing γ away from the surface as shown in fig. 2. Also, a cross over is found in the nanofluid concentration boundary layers as shown in fig. 4. For the dynamic region (close to the surface), the increase of γ leads to a decrease in the concentration boundary layers slightly due to the little enhancement of the surface mass flux.

According to eqs. (8) and (9), the coefficient $(1 + 2\gamma\eta)$ controls the thermal and the mass diffusions of the nanofluid. So the increase of γ away from the cylinder surface improves the thermal and the mass diffusion of the temperature from the cylinder surface to the nanofluid, hence the nanofluid temperature and concentration increases as shown in figs. 3 and 4.

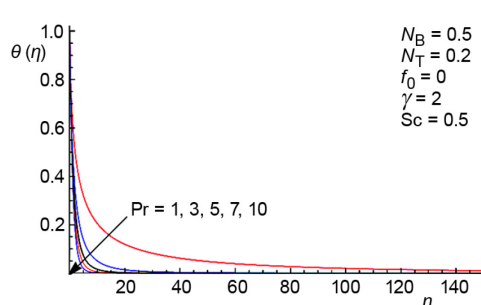


Figure 5. The temperature profiles for various values of Pr

Prandtl number

From tab. 2, the surface shear stress (skin friction) is not influenced by any change in the Prandtl number, so the nanofluid velocity is not affected too. For small values of Prandtl number, the surface heat flux (Nusselt number) is increased and the surface mass flux (Sherwood number) is decreased while the reverse takes place for the large values of Prandtl number.

From fig. 5, the nanofluid temperature profiles are decreased by increasing the values

of Prandtl number. A good explanation of this observation is that the nanofluid with the highest Prandtl number has the lowest thermal conductivity (or the highest viscosity). Thereby, the nanofluid thermal boundary layers will be the thinner.

A cross-over is found in the nanofluid concentration boundary layers as shown in fig. 6. For the dynamic region (close to the surface), the increase of Prandtl number leads to an increase in the concentration boundary layers slightly. Away from the surface, the reverse takes place.

Brownian diffusion

Brownian diffusion is the random moving of nanoparticles suspended in a fluid resulting from their bombardment by the fast moving atoms or molecules in the fluid. This motion controls the temperature and the concentration of the particles within the boundary layer over the surface. The Brownian motion parameter, N_B , is the key of this motion.

From tab. 2, the surface shear stress (skin friction) is not influenced by any change in the Brownian diffusion parameter, N_B , so the nanofluid velocity is not affected too. The surface heat flux (Nusselt number) is decreased and the nanofluid temperature is increased by increasing N_B as shown in tab. 2 and fig. 7. An interpretation of these observations is that the nanofluid with the lowest Brownian diffusion parameter has the highest volumetric heat capacity. Hence, the heat flux transferred from the surface to the nanofluid is increased and the surface is cooled off.

On the other hand, the surface mass flux (Sherwood number) is increased and the nanofluid concentration is decreased by increasing N_B as seen from tab. 2 and fig. 8. This phenomenon is interpreted by the fact that the enhancement of the Brownian diffusion will increase the random motion of the nanoparticles to scatter from the nanofluid (higher concentration zone) toward the cylinder surface (lower concentration zone).

Thermophoresis

Thermophoresis is a phenomenon observed in mixtures of mobile particles where the different particle types exhibit different responses to the force of a temperature gradient.

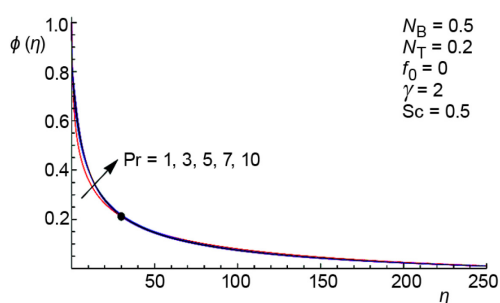


Figure 6. The concentration profiles for various values of Pr

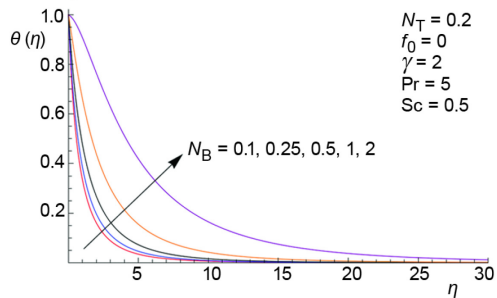


Figure 7. The temperature profiles for various values of N_B

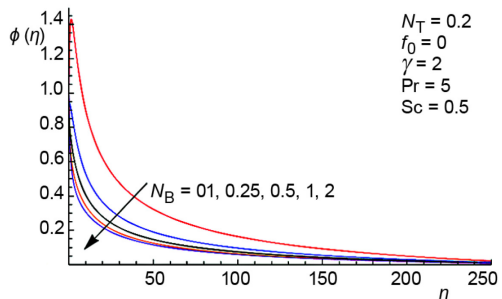


Figure 8. The concentration profiles for various values of N_B

Explaining this phenomenon appears in this study through the thermophoresis parameter, N_T . It is worth mentioning that the thermophoresis parameter is possible to be a positive or negative where the negative value of N_T indicates to hot surface while positive one indicates to cold surface. Moreover for hot surfaces, thermophoresis tends to blow the nanoparticles concentration boundary layer away from the surface since a hot surface repels the nanoparticles from it. Thereby, a relatively nanoparticles free layer is formed close to the surface.

From tab. 2, the surface shear stress (skin friction) is not influenced by any change in the thermophoresis diffusion parameter, N_T , so the nanofluid velocity is not affected too. The surface heat flux (Nusselt number) is decreased and the nanofluid temperature is increased by increasing N_T as shown in tab. 2 and fig. 9. An interpretation of these observations is that the lower thermophoresis diffusion parameter nanofluid has a higher volumetric heat capacity. Hence, the heat flux transferred from the surface to the nanofluid is increased and the surface is cooled off.

On the other hand, the surface mass flux (Sherwood number) is increased and the nanofluid concentration is increased by increasing N_T as seen from tab. 2 and fig. 10. This phenomenon is interpreted by the fact that the enhancement of the thermophoresis diffusion will increase the random motions of the nanoparticles to scatter from the cylinder surface (higher temperature zone) toward the nanofluid (lower temperature zone).

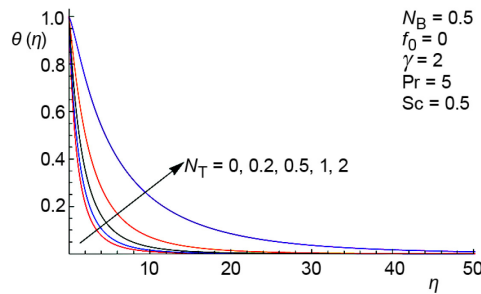


Figure 9. The temperature profiles for various values of N_T

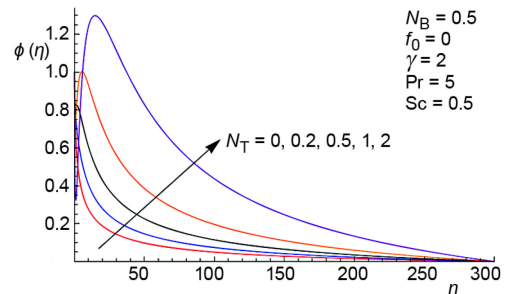


Figure 10. The concentration profiles for various values of N_T

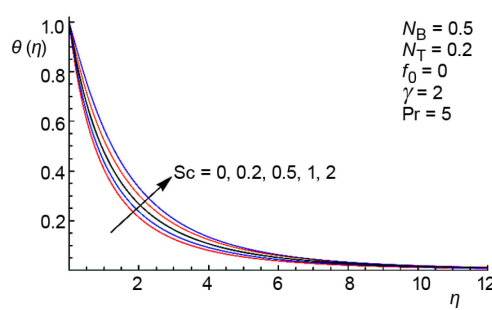


Figure 11. The temperature profiles for various values of Sc

On the other hand, the surface mass flux (Sherwood number) is increased and the nanofluid concentration is increased by increasing Schmidt number as seen from tab. 2 and

Schmidt number

From tab. 2, the surface shear stress (skin friction) is not influenced by any change in the Schmidt number, so the nanofluid velocity is not affected too. The surface heat flux (Nusselt number) is decreased and the nanofluid temperature is increased by increasing Schmidt number as shown in tab. 2 and fig. 11. An interpretation of these observations is that the lower Schmidt number nanofluid has a lower Brownian diffusion coefficient hence the heat flux transferred from the surface to the nanofluid is increased and the surface is cooled off.

fig. 12. This phenomenon is interpreted by the fact that the enhancement of the Schmidt number increases the Brownian diffusion.

Suction/injection velocity

The suction/injection parameter, f_0 , can play a crucial role to control the friction between the nanofluid and the surface which influences the heat transfer rate at the surface. Physically, suction causes the nanofluid streamlines to adhere more closely to the surface. Thereby, the surface shear stress (skin friction) increases as seen from tab. 2. Accordingly, the frictional forces between the nanofluid layers increase and cause the nanofluid velocity to slow down as recognized from fig. 13. On the other hand, the reverse behaviour is noticed for the case of injection.

According to tab. 2 and fig. 14, the nanofluid temperature is increased during the injection process compared to the suction one. Consequently, the surface heat flux (Nusselt number) is decreased during the injection process and the reverse happens in the suction one. The physical interpretation of this phenomenon is that the lateral mass flux through the cylinder during the injection process enhances the thermal conductivity of the nanofluid. Thereby, the amount of temperature poured from the surface to the nanofluid is increased and the surface heat flux (Nusselt number) is decreased. The reverse takes place in the suction process.

A cross over is also found in the nanofluid concentration boundary layers as shown in fig. 15. For the dynamic region (close to the surface), the suction process leads to an increase in the concentration boundary layers slightly while the injection one decreases the concentration boundary layers. The reverse takes place away from the surface.

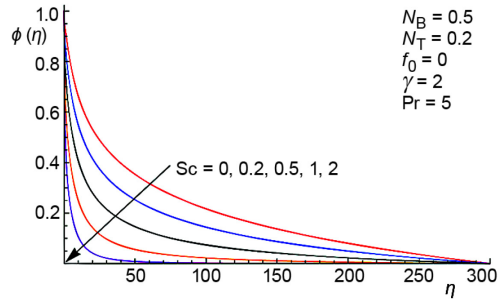


Figure 12. The concentration profiles for various values of Sc

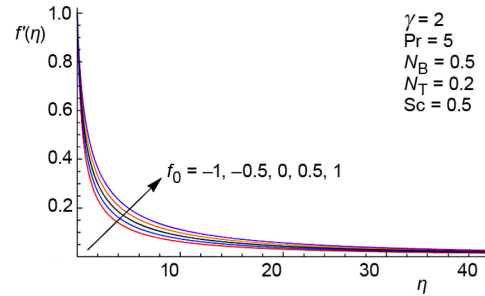


Figure 13. The velocity profiles for various values of f_0

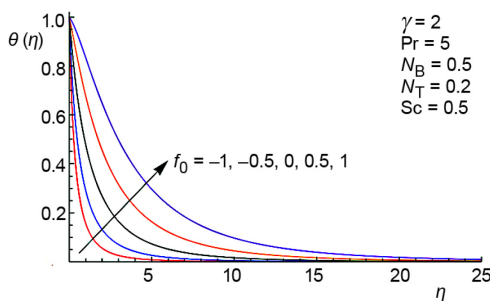


Figure 14. The temperature profiles for various values of f_0

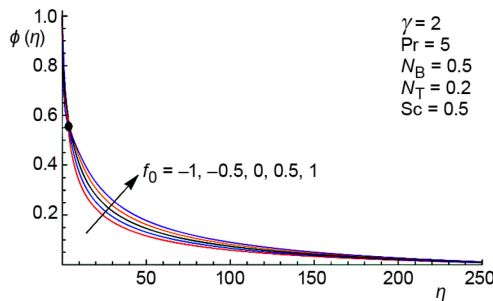


Figure 15. The concentration profiles for various values of f_0

Conclusions

Numerical solutions have been obtained for the laminar boundary layer flow of nanofluid along a horizontal cylinder affected by Brownian and thermophoresis motions in the presence of suction/injection velocity. An appropriate similarity transforms were used to transform the momentum and the energy equations into a set of ordinary differential equations which are solved by using MATHEMATICA. Numerical computations show that the present values of the rate of heat transfer are in a great agreement with those obtained by previous investigations. The following results are obtained.

- The nanofluid velocity, temperature, and concentration increase with the increase in the curvature parameter far from the stretching surface while they show the reverse near the stretching surface.
- The nanofluid temperature decrease with the increase in the Prandtl number. Also, the nanofluid concentration decrease with the increase in the Prandtl number far from the stretching surface while they show the reverse near the stretching surface.
- The nanofluid temperature increases with the increase in the Brownian diffusion, the thermophoresis diffusion, and the Schmidt number.
- The nanofluid concentration increases with the increase in the thermophoresis parameter but it decreases with the increase in the Brownian diffusion parameter and the Schmidt number.
- The nanofluid velocity and temperature are increased in the injection process compared to the suction one.
- Close to the surface, the suction process leads to an increase in the concentration boundary layers slightly while the injection one decreases the concentration boundary layers. The reverse takes place away from the surface.
- The surface hardness and strength are improved by decreasing the radius of the cylinder but on the other hand the surface shear stress is increased.
- The surface hardness and strength are improved by decreasing the Prandtl and Schmidt numbers and the Brownian and the thermophoresis diffusions while the surface shear stress is not influenced.
- The surface hardness and strength are enhanced in the suction case compared to the injection one. The surface shear stress is decreased in the injection process compared to the suction one.

Nomenclature

a	- cylinder radius, [m]	q_w	- surface heat flux, [W m^{-2}]
C	- specific heat capacity, [J K^{-1}]	Re	- Reynolds number ($= \ell U_w / v$), [-]
C_f	- local skin friction coefficient ($= 2\tau_w \rho U_w^2$), [-]	Sc	- Schmidt number ($= D_B / v$), [-]
D_B	- Brownian diffusion coefficient, [$\text{m}^2 \text{s}^{-1}$]	Sh_x	- local Sherwood number ($= x Q_w / \kappa \Delta \phi$), [-]
D_T	- thermophoresis coefficient, [$\text{m}^2 \text{s}^{-1}$]	T	- nanofluid temperature, [K]
f	- dimensionless stress, [-]	T_w	- surface temperature, [K]
f_0	- suction/injection parameter $[= (\ell/vU_0)^{1/2} V]$, [ms^{-1}]	T_∞	- nanofluid ambient temperature, [K]
N_B	- Brownian diffusion parameter $[= (\rho C)_p D_B \Delta \phi / \rho C]$, [$\text{m}^2 \text{s}^{-1}$]	u	- nanofluid velocity along the x-axis, [ms^{-1}]
N_T	- thermophoresis parameter $[= (\rho C)_p D_T \Delta T / \rho C T_\infty]$, [$\text{m}^2 \text{s}^{-1}$]	U_w	- surface velocity ($= U_0 x / \ell$), [ms^{-1}]
Nu_x	- local Nusselt number ($= x q_w / \kappa \Delta T$), [-]	U_0	- reference velocity, [ms^{-1}]
Pr	- Prandtl number ($= v/\alpha$), [-]	v	- nanofluid velocity along the r-axis, [ms^{-1}]
Q_w	- surface mass flux, [$\text{Kmol m}^{-2} \text{s}^{-1}$]	V	- suction/injection velocity, [ms^{-1}]
		r	- radial co-ordinate perpendicular to the cylinder axis, [m]
		x	- axial co-ordinate of the cylinder, [m]

Greek symbols

α	– thermal diffusivity, [m^2s^{-1}]
γ	– curvature parameter [= $a^{-1}(v\ell/U_0)^{1/2}$], [-]
η	– dimensionless variable [= $(r^2 - a^2)(U_w/vx)^{1/2}/2a$], [m]
θ	– dimensionless temperature function [= $(T - T_\infty)/\Delta T$], [-]
κ	– thermal conductivity, [$\text{W m}^{-1}\text{K}^{-1}$]
μ	– dynamic viscosity, [$\text{Pa}\cdot\text{s}$]
ν	– kinematic viscosity, [m^2s^{-1}]
ρ	– mass density, [kg m^{-3}]
τ_w	– surface shear stress, [$\text{kg m}^{-1}\text{s}^{-2}$]
φ	– nanoparticle concentration, [mol m^{-3}]

ϕ – dimensionless concentration function
[= $(\varphi - \varphi_\infty)/\Delta\varphi$], [-]

ψ – stream function
[= $a(U_w vx)^{1/2} f(\eta)$], [m^3s^{-1}]

ℓ – characteristic length (= $2a$), [m]

Superscript

' – differentiation with respect to η

Subscripts

p	– nanoparticles conditions
w	– stretching surface conditions
0	– nanofluid reference conditions
∞	– nanofluid ambient conditions

References

- [1] Schlichting, H., *Boundary Layer Theory*, 6th ed, McGraw-Hill, New York, USA, 1968
- [2] Sakiadis, B. C., Boundary Layer Behavior on Continuous Solid Surfaces: I. Boundary Layer Equations for Two Dimensional and Axisymmetric Flow, *AICHE J.*, 7 (1961), 2, pp. 26-28
- [3] Sakiadis, B. C., Boundary Layer Behaviour on Continuous Solid Surfaces: II. Boundary Layer Equations on a Continuous Flat Surface, *AICHE J.*, 7 (1961), 2, pp. 221-225
- [4] Crane, L. J., Flow Past a Stretching Plane, *Z. Angew. Math. Phys.*, 21 (1970), 4, pp. 645-647
- [5] Vleggaar, J., Laminar Boundary Layer Behaviour on Continuous Accelerating Surfaces, *Chem. Eng. Sci.*, 32 (1977), 12, pp. 1517-1525
- [6] Gupta, P. S., Gupta, A. S., Heat and Mass Transfer on a Stretching Sheet with Suction or Blowing, *Can. J. Chem. Eng.*, 55 (1977), 6, pp. 744-746
- [7] Soundalgekar, V. M., Ramana, T. V., Heat Transfer Past a Continuous Moving Plate with Variable Temperature, *Waerme- und Stoffübertragung*, 14 (1980), 2, pp. 91-93
- [8] Lin, H. T., Shih Y. P., Laminar Boundary Layer Heat Transfer along Static and Moving Cylinder, *J. Chin. Inst. Eng.*, 3 (1980), 1, pp. 73-79
- [9] Lin, H. T., Shih, Y. P., Buoyancy Effects on the Laminar Boundary Layer Heat Transfer along Vertically Moving Cylinder, *J. Chin. Inst. Eng.*, 4 (1981), 1, pp. 47-51
- [10] Banks, W. H. H., Similarity Solutions of the Boundary Layer Equation for a Stretching Wall, *J. Mech. Theo. Appl.*, 2 (1983), 3, pp. 375-392
- [11] Grubka, L. J., Bobba, K. M., Heat Transfer Characteristics of a Continuous Stretching Surface with Variable Temperature, *J. Heat Transfer*, 107 (1985), 1, pp. 248-250
- [12] Wang, C. Y., Fluid Flow Due to a Stretching Cylinder, *Phys. of Fluids*, 31 (1988), 3, pp. 466-468
- [13] Wang, C. Y., Free Convection on a Vertical Stretching Surface, *J. of App. Math and Mech.*, 69 (1989), 11, pp. 418-420
- [14] Ali, M. E., Heat Transfer Characteristics of a Continuous Stretching Surface, *Waerme- und Stoffübertragung*, 29 (1994), 4, pp. 227-234
- [15] Ali, M. E., On Thermal Boundary Layer on a Power Law Stretched Surface with Suction or Injection, *Int. J. Heat Fluid Flow*, 16 (1995), 4, pp. 280-290
- [16] Elbashbeshy, E. M. A., Heat Transfer over a Stretching Surface with Variable Heat Flux, *J. Phys. D: Appl. Phys.*, 31 (1998), 16, pp. 1951-1955
- [17] Raptis, A., Radiation and Free Convection Flow through a Porous Medium, *Int. Comm. in Heat and Mass Transf.*, 25 (1998), 2, pp. 289-295
- [18] Takhar, H. S., et al., Natural Convection on a Vertical Cylinder Embedded in a Thermally Stratified High Porosity Medium, *Int. J. of Thermal Science*, 41 (2002), 1, pp. 83-93
- [19] Ishak, A., et al., Unsteady Mixed Convection Boundary Layer Flow due to a Stretching Vertical Surface, *Arab J. for Sci. and Eng.*, 31 (2006), 2, pp. 165-182
- [20] Ishak, A., et al., Magnetohydrodynamic (MHD) Flow and Heat Transfer due to a Stretching Cylinder, *Energy Conversion and Management*, 49 (2008), 11, pp. 3265-3269
- [21] Molla, Md. M., et al., Natural Convection Flow from a Horizontal Cylinder with Uniform Heat Flux in Presence of a Heat Generation, *Appl. Math. Modelling*, 33 (2009), 7, pp. 3226-3236

- [22] Bachok, N., Ishak, A., Mixed Convection Boundary Layer Flow over a Vertical Cylinder with a Prescribed Surface Heat Flux, *European J. of Scientific Research*, 34 (2009), 1, pp. 46-54
- [23] Ishak, A., Nazar, R., Laminar Boundary Layer Flow along a Stretching Cylinder, *European J. of Scientific Research*, 36 (2009), 1, pp. 22-29
- [24] Elbashbeshy, E. M. A., Aldawody, D. A., Effects of Thermal Radiation and Magnetic Field on Unsteady Mixed Convection Flow and Heat Transfer over a Porous Stretching Surface in the Presence of Internal Heat Generation/Absorption, *Int. J. of the Phys. Sci.*, 6 (2011), 6, pp. 1540-1548
- [25] Elbashbeshy, E. M. A., et al., Effect of Magnetic Field on Flow and Heat Transfer over a Stretching Horizontal Cylinder in the Presence of a Heat Source/Sink with Suction/Injection, *J. of Applied Mechanical Engineering*, 1 (2012), 1, pp. 1-5
- [26] Elbashbeshy, E. M. A., et al., Laminar Boundary Layer Flow along a Stretching Cylinder Embedded in a Porous Medium, *International J. of Physical Sciences*, 7 (2012), 24, pp. 3067-3072
- [27] Elbashbeshy, E. M. A., et al., Laminar Boundary Layer Flow along a Stretching Horizontal Cylinder Embedded in a Porous Medium in the Presence of a Heat Source or Sink with Suction/Injection, *International J. of Energy and Technology*, 4 (2012), 28, pp. 1-6
- [28] Masuda, et al., Alteration of Thermal Conductivity and Viscosity of Liquid by Dispersing Ultra-Fine Particles, *Netsu Bussei*, 7 (1993), 4, pp. 227-233
- [29] Choi, S. U. S., Enhancing Conductivity of Fluids with Nanoparticles, *Proceedings*, ASME International Mechanical Engineering Congress and Exposition, San Francisco, Cal., USA, 1995, pp. 99-105
- [30] Choi, S. U. S., et al., Anomalously Thermal Conductivity Enhancement in Nanotube Suspension, *Appl. Phys. Lett.*, 79 (2001), 14, pp. 2252-2254
- [31] Buongiorno, J., Convective Transport in Nanofluids, *ASME J. Heat Transf.*, 128 (2006), 3, pp. 240-250
- [32] Das, S. K., et al., *Nanofluids: Science and Technology*, Wiley Interscience, N. J., USA, 2007
- [33] Kakac, S., Pramuanjaroenkij, A., Review of Convective Heat Transfer Enhancement with Nanofluids, *Int. J. of Heat and Mass Transf.*, 52 (2009), 13, pp. 3187-3196
- [34] Bachok, N., et al., Boundary-Layer Flow of Nanofluids over a Moving Surface in a Flowing Fluid, *Int. J. of Thermal Sci.*, 49 (2010), 9, pp. 1663-1668
- [35] Khan, W. A., Pop, I., Boundary-Layer Flow of Nanofluid past a Stretching Sheet, *Int. J. of Heat and Mass Transf.*, 53 (2010), 11, pp. 2477-2483
- [36] Hamad, M. A. A., Analytical Solution of Natural Convection Flow of Nanofluid over a Linearly Stretching Sheet in the Presence of Magnetic Field, *Int. Comm. in Heat and Mass Transf.*, 38 (2011), 4, pp. 487-492
- [37] Nazar, R., et al., Mixed Convection Boundary Layer Flow from a Horizontal Circular Cylinder Embedded in a Porous Medium Filled with a Nanofluid, *Transport in Porous Media*, 86 (2011), 2, pp. 517-536
- [38] Bachok, N., et al., Boundary Layer Flow over a Moving Surface in a Nanofluid with Suction or Injection, *Acta Mech. Sin.*, 28 (2012), 1, pp. 34-40
- [39] Hamad, M. A. A., Ferdows, M., Similarity Solutions to Viscous Flow and Heat Transfer of Nanofluid over Nonlinearly Stretching Sheet, *Appl. Math Mech. Eng.*, 33 (2012), 7, pp. 923-930
- [40] Tham, L., et al., Mixed Convection Boundary Layer Flow from a Horizontal Circular Cylinder in a Nanofluid, *Int. J. of Numerical Methods for Heat & Fluid Flow*, 22 (2012), 5, pp. 576-606
- [41] Rabeti, M., et al., Forced Convection Heat Transfer over a Horizontal Plate Embedded in a Porous Medium Saturated with a Nanofluid in the Presence of Heat Sources, *Advances in Energy Eng. (AEE)*, 1 (2013), 2, pp. 46-51
- [42] Elbashbeshy, E. M. A., et al., Effect of Heat Treatment Process with a New Cooling Medium (Nanofluid) on the Mechanical Properties of an Unsteady Continuous Moving Cylinder, *J. of Mechanical Science and Technology*, 27 (2013), 12, pp. 3843-3850
- [43] Habibi Matin, M., Jahangiri, P., Forced Convection Boundary Layer Magnetohydrodynamic Flow of Nanofluid over a Permeable Stretching Plate with Viscous Dissipation, *Thermal Science*, 18 (2014), Suppl. 2, pp. S587-S598
- [44] Bogacki, P., Shampine, L. F., An Efficient Runge-Kutta (4,5) Pair, *Computers & Mathematics with Applications*, 32 (1996), 6, pp. 15-28